Proceedings of the 2005 IEEE/ASME
International Conference on Advanced Intelligent Mechatronics
Monterey, California, USA, 24-28 July, 2005

A New Continuously Differentiable Friction Model for Control Systems Design

C. Makkar, W. E. Dixon, W. G. Sawyer, and G.Hu
Mechanical and Aerospace Engineering
University of Florida, Gainesville, FL 32608
Email:cmakkar, wdixon, wgsawyer, gqhu@ufl.edu.

***Abstract*— For high-performance engineering systems, model-based controllers are typically required to accommodate for the system nonlinearities. Unfortunately, developing accurate models for friction has been historically challenging. Typical models are either discontinuous and many other models are only piecewise continuous. Motivated by the fact that discontinuous and piecewise continuous friction models are problematic for the development of high-performance continuous controllers, a new model for friction is proposed in this paper. This simple continuously differentiable model represents a foundation that captures the major effects reported and discussed in friction modeling and experimentation. The proposed model is generic enough that other subtleties such as frictional anisotropy with sliding direction can be addressed by mathematically distorting this model without compromising the continuous differentiability.**

I. Introduction

General Euler-Lagrange systems can be described by the following nonlinear dynamic model:

$$M(q)\ddot{q} + V_m(q,\dot{q})\dot{q} + G(q) + f(\dot{q}) = \tau(t). \qquad (1)$$

In (1), $M(q) \in \mathbb{R}^{n\times n}$ denotes the inertia matrix, $V_m(q,\dot{q}) \in \mathbb{R}^{n\times n}$ denotes the centripetal-Coriolis matrix, $G(q) \in \mathbb{R}^n$ denotes the gravity vector, $f(\dot{q}) \in \mathbb{R}^n$ denotes a friction vector, $\tau(t) \in \mathbb{R}^n$ represents the torque input control vector, and $q(t)$, $\dot{q}(t)$, $\ddot{q}(t) \in \mathbb{R}^n$ denote the link position, velocity, and acceleration vectors, respectively. For high-performance engineering systems, model-based controllers [6] are typically required to accommodate for the system nonlinearities. In general, either accurate models of the inertial effects can be developed or numerous continuous adaptive and robust control methods can be applied to mitigate the effects of any potential mismatch in the inertial parameters. Unfortunately, developing accurate models for friction has been historically problematic. In fact, after decades of theoretical and experimental investigation, a general model for friction has not been universally accepted, especially at low speeds where friction effects are exaggerated. In fact, [1] examined the destabilizing effects of certain friction phenomena (i.e., the Stribeck effect) at low speeds. To further complicate the development of model-based controllers for high-performance systems, friction is often modeled as discontinuous; thus, requiring a discontinuous controller to compensate for the effects.

Motivated by the desire to develop an accurate representation of friction in systems, various control researchers have developed different analytical models, estimation methods to identity friction effects, and adaptive and robust methods to compensate for or reject the friction effects. In general, the dominant friction components that have been modeled include: *Static friction* (i.e., the torque that opposes the motion at zero velocity), *Coulomb friction* (i.e., the constant motion opposing torque at non-zero velocity), *Viscous friction* (i.e., when full fluid lubrication exists between the contact surfaces), *Asymmetries* (i.e., different friction behavior for different directions of motion), *Stribeck effect* (i.e., at very low speed, when partial fluid lubrication exists, contact between the surfaces decreases and thus friction decreases exponentially from stiction), *Position dependence* (oscillatory behavior of the friction torque due to small imperfections on the motor shaft and reductor centres, as well as ball bearings elastic deformation).

Classical friction models were derived from static maps between velocity and friction force. From comprehensive surveys of friction models in literature (see [1] and [2]), modern researchers have concluded that dynamic friction effects are necessary to complete the friction model. Several dynamic friction models have been proposed (see [4] and [5]). These models combine the Dahl model [7] with the arbitrary steady-state friction characteristics of the bristle-based LuGre model proposed by Canudas de Wit et al. in [5]. A recent modification to the LuGre model is given in the Leuven model [12]. The Lueven model was later experimentally confirmed in [9]. However, a modification to the Leuven model is provided in [11] that replaces the stack mechanism used to implement the hysteresis by the more efficient Maxwell slip model. Another criticism to the LuGre model has been recently raised by Dupont et al. [8], who underline a nonphysical drift phenomenon that arises when the applied force is characterized by small vibrations below the static friction limit. Recently single and multistate integral friction models have been developed [10] based on the integral solution of the Dahl model. However, these friction models are based on the assumption that the friction coefficient is constant with sliding speed and have a singularity at the onset of slip. Unfortunately, each of the aforementioned models are discontinuous (i.e., a signum

function of the velocity is used to assign the direction of friction force such as [8], [10], [11], and [12]), and many other models are only piecewise continuous (e.g., the LuGre model in [5]). As stated previously, the use of discontinuous and piecewise continuous friction models is problematic for the development of high-performance continuous controllers.

The efforts in this paper provide a first step at creating a continuously differentiable friction model that captures a number of essential aspects of friction without involving discontinuous or piecewise continuous functions. This simple continuously differentiable model represents a foundation that captures the major effects reported and discussed in friction modeling and experimentation. The proposed model is generic enough that other subtleties such as frictional anisotropy with sliding direction can be addressed by mathematically distorting this model without compromising the continuous differentiability. The friction model and the associated properties are provided in Section 2. The generality of the model is demonstrated through a numerical simulation in Section 3. Specifically, numerical simulations are provided for different friction model parameters to illustrate the different effects that the model captures.

II. Friction Model and Properties

The friction term $f(\dot{q})$ in (2) is assumed to have the following non-linear parameterizable form:

$$f(\dot{q}) = \gamma_1(\tanh(\gamma_2\dot{q}) - \tanh(\gamma_3\dot{q})) + \gamma_4 \tanh(\gamma_5\dot{q}) + \gamma_6\dot{q} \quad (2)$$

where $\gamma_i \in \mathbb{R}\ \forall i = 1, 2, ...6$ denote unknown positive constants. The friction model in (2) has the following properties.

- Friction model is symmetric about the origin.
- The static coefficient of friction can be approximated by the term $\gamma_1 + \gamma_4$.
- The term $\tanh(\gamma_2\dot{q}) - \tanh(\gamma_3\dot{q})$ captures the Stribeck effect where the friction coefficient decreases from the static coefficient of friction with increasing slip velocity near the origin.
- A viscous dissipation term is given by $\gamma_6\dot{q}$.
- The Coulombic friction coefficient is present in the absence of viscous dissipation and is modelled by the term $\gamma_4 \tanh(\gamma_5\dot{q})$.
- The friction model is dissipative in the sense that a passive operator $\dot{q}(t) \rightarrow f(\cdot)$ satisfies the following integral inequality [3]

$$\int_{t_0}^{t} \dot{q}(\tau) f(\dot{q}(\tau)) d\tau \geq -c^2$$

where c is a positive constant, provided $\dot{q}(t)$ is bounded.

Figs. 1 and 2 illustrate the sum of the different effects and characteristics of the friction model. Fig. 3 shows the flexibility of such a model.

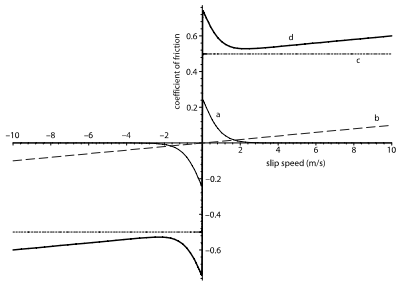

Fig. 1. Friction model as a composition of different effects including: a) Stribeck effect, b) viscous dissipation, c) Coulomb effect, and d) the combined model.

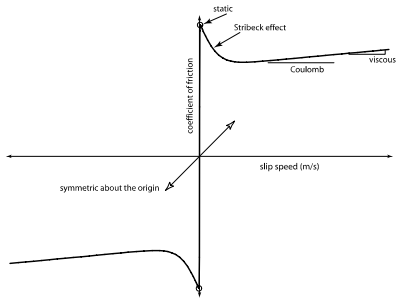

Fig. 2. Characteristics of the Friction model.

III. Stick-Slip Simulation

The qualitative mechanisms of friction are well-understood. To illustrate how the friction model presented in 2 exhibits these effects, various numerical simulations are presented in this section. The system considered in Fig. 4 is a simple mass-spring system, in which a unit mass M is attached to a spring with stiffness k resting on a plate moving with a velocity V_p in the forward direction, which causes the block to move with a velocity V_b. The modelled system can be compared to a mass attached to a fixed spring moving on a conveyor belt. The plate is moving with a velocity that slowly increases and saturates, given by the following relation:

$$V_p = 1 - e^{-at}.$$

The time delay constant for all the numerical simulations was selected as $a = 0.1$. Fig. 5 shows the plate velocity as a function of time.

The system described by Fig. 4 is modelled as follows:

$$M\ddot{x}_b(t) + kx_b(t) - Mgf(\dot{x}_p(t) - \dot{x}_b(t)) = 0$$

where the term $\dot{x}_p(t) - \dot{x}_b(t)$ represents the slip velocity, (i.e., the difference between the plate velocity and block velocity at any instant of time). To demonstrate the flexibility of the model, model parameters were varied in order to capture the Stribeck effect, Coulombic friction effect and viscous dissipation. For example, hydrodynamic lubrication in many operating regimes is viscous, lacking the other effects, which are easily set to zero in the model. Simple Coulombic friction models are often good for solid lubricant coatings at moderate

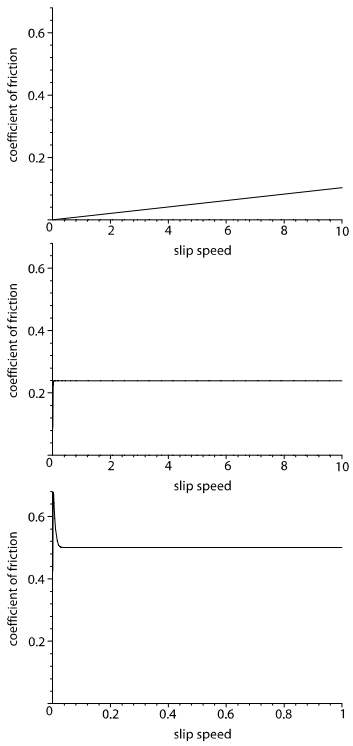

Fig. 3. Modular ability of the model to selectively model different friction regimes: top plot - viscous regime (e.g., hydrodynamic lubrication), middle plot - Coulombic friction regime (e.g., solid lubricant coatings at moderate sliding speeds), and bottom plot - abrupt change from static to kinetic friction (e.g., non-lubricous polymers).

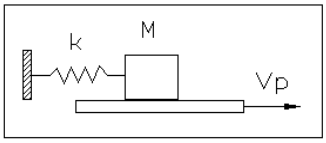

Fig. 4. Mass-spring system for demonstrating stick-slip friction.

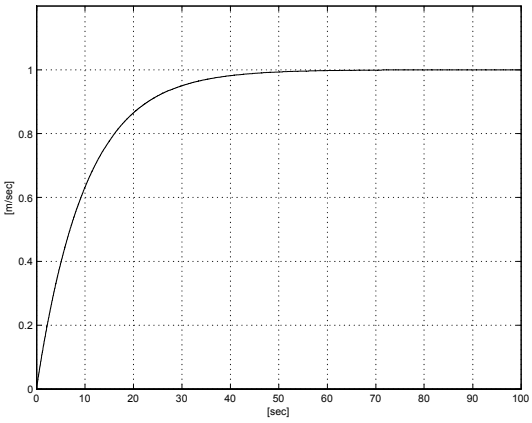

Fig. 5. Plate velocity vs time.

sliding speeds. To capture this effect, the static and viscous terms can be set to zero. For some sticky or non-lubricous polymers, there exists an abrupt change from static to kinetic friction, which is captured by making the Stribeck decay very rapid.

A Coulombic friction regime is displayed in Fig. 9 where the friction model parameters are set as follows: $\gamma_1 = 0$, $\gamma_2 = 0$, $\gamma_3 = 0$, $\gamma_4 = 0.1$, $\gamma_5 = 100$, $\gamma_6 = 0$. The block velocity, slip velocity, and the friction force as a function of time can be seen in Figs. 6 - 8. These figures indicate that the block velocity slowly rises, reaches a maximum and then begins to oscillate. The slip velocity also rises and then oscillates after reaching a maximum value. The Coulombic friction coefficient is a constant opposing the motion of the block as seen in Figs. 8 and 9. These figures indicate that the friction force causes the block to move along with the plate until the spring force overcomes the friction force; hence, the block begins to slip in an opposite direction of the plate velocity causing the spring to compress. As the spring releases energy back into the system, the block velocity exceeds the plate velocity. The magnitude of the constant friction coefficient results in a constant oscillation between the friction force and the spring force.

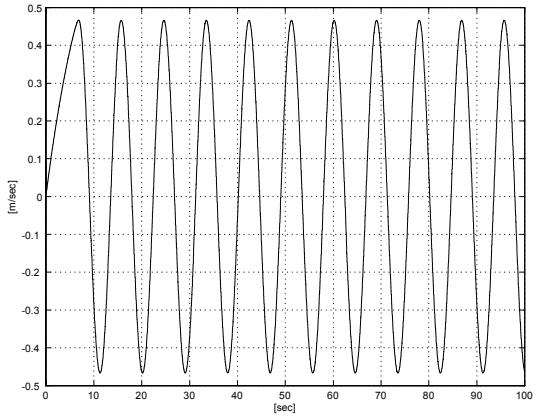

Fig. 6. Block velocity vs time.

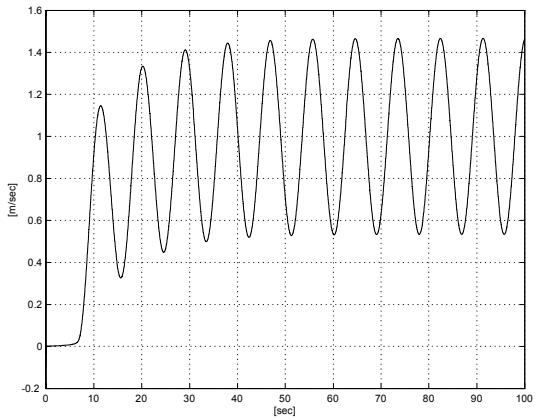

Fig. 7. Slip velocity vs time.

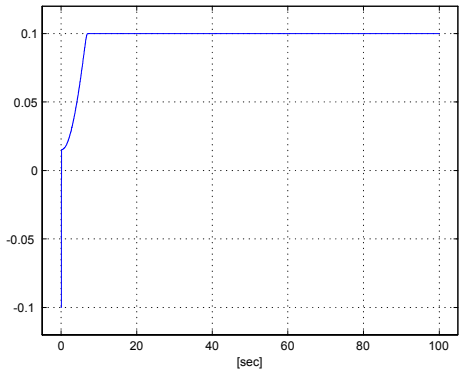

Fig. 8. Friction coefficient vs time.

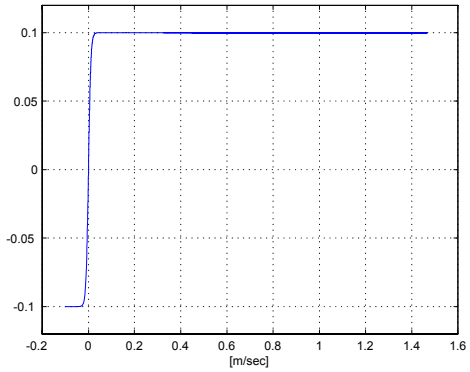

Fig. 9. Friction coefficient vs slip velocity.

To illustrate the viscous friction regime, the parameters were set as follows: $\gamma_1 = 0$, $\gamma_2 = 0$, $\gamma_3 = 0$, $\gamma_4 = 0$, $\gamma_5 = 0$, $\gamma_6 = 0.01$. The block velocity, slip velocity and the friction force can be seen as the function of time in Figs. 10 - 12. The block velocity in Fig. 10 slowly decreases as the viscous friction increases as displayed in Fig. 13. The viscous coefficient of friction is an order of magnitude smaller in comparison to the Coulombic friction coefficient, as a result the friction force is not sufficient enough to sustain the oscillations of the block. The block eventually comes to rest and constantly slips on the moving plate.

The Stribeck effect is modeled using the following friction model parameter values: $\gamma_1 = 0.25$, $\gamma_2 = 100$, $\gamma_3 = 10$, $\gamma_4 = 0$, $\gamma_5 = 0$, $\gamma_6 = 0$. The block velocity, slip velocity and the friction force are plotted as functions of time in Figs. 14 - 16. As seen in Fig. 17, the Stribeck effect is seen as the high breakaway force at the beginning of the motion of the block, which then exponentially decreases. The block moves with the plate due to the initial friction force. Eventually enough energy is stored in the spring so that the spring force overcomes the breakaway friction. The friction force exponentially decays after the breakaway force is reached. After the block overcomes the breakaway force, the spring

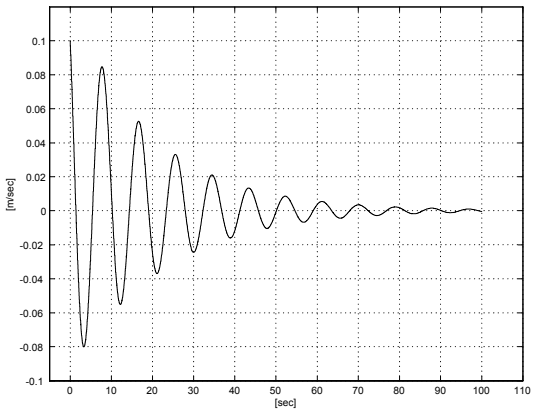

Fig. 10. Block velocity vs time.

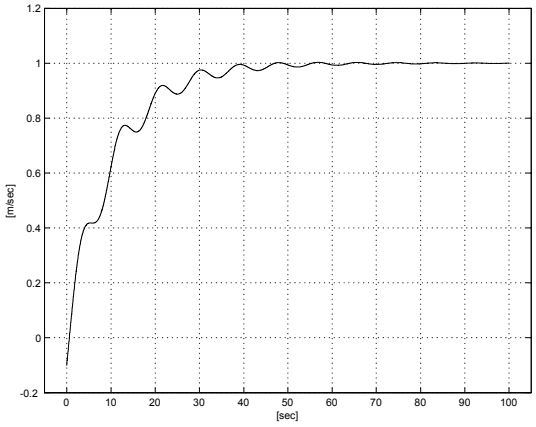

Fig. 11. Slip velocity vs time.

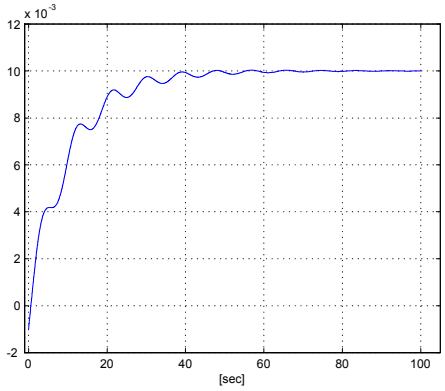

Fig. 12. Friction coefficient vs time.

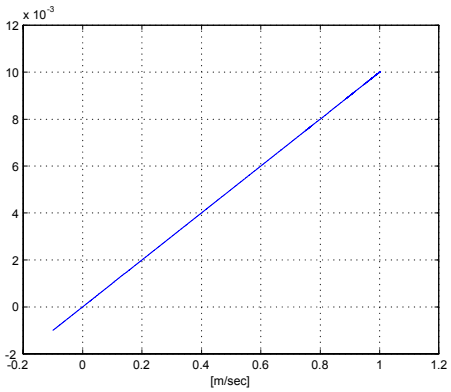

Fig. 13. Friction coefficient vs slip velocity.

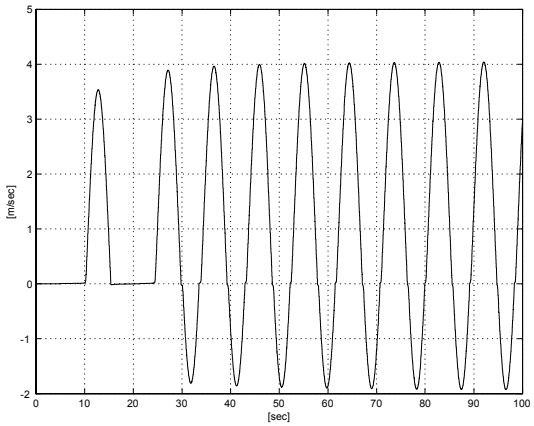

Fig. 15. Slip velocity vs time.

force becomes dominant and causes the block to reverse its direction and move towards the spring. Since there is no force opposing this motion, a large slip velocity is exhibited while the spring compresses and releases, pushing the block faster than the plate.

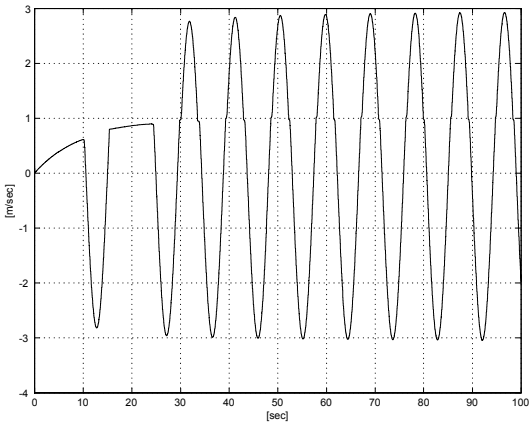

Fig. 14. Block velocity vs time.

Fig. 21 illustrates the sum of the different effects in the friction model in a stick-slip regime with the following friction model parameters $\gamma_1 = 0.25$, $\gamma_2 = 100$, $\gamma_3 = 10$, $\gamma_4 = 0.1$, $\gamma_5 = 100$, $\gamma_6 = 0.01$. Figs. 18 - 20 show the velocity of the block, slip velocity and friction force as the function of time. The velocity of block slowly increases as the plate moves, reaches a maximum value where the spring reaches its maximum extension. At this point, the spring pulls the block back, reversing the direction of the block velocity and hence causing the block to oscillate.

IV. Conclusion

Motivated by the fact that discontinuous and piecewise continuous friction models are problematic for the development of high-performance continuous controllers, a new model for friction is proposed in this paper. The simple continuously differentiable model was shown to exhibit viscous, Coulombic, static, and Stribeck effects, and is inherently passive. A numerical simulation demonstrates the modularity of the model for use in different friction regimes. A significant advantage of the proposed model is that the model supports the development of differentiable model-based controllers. Future efforts will focus on 1) matching experimental data to the analytical model, 2) expanding/adjusting the model to exhibit additional effects, and 3) developing new controllers that compensate for the friction effects.

References

[1] B. Armstorng -Helouvry, *Control of Machines with Friction*, Boston, MA, Kluwer, 1991.

[2] B. Armstorng -Helouvry, P. Dupont, and C. Canudas de Wit, "A Survey of Models, Analysis Tools and Compensation Methods for the Control of Machines with Friction," *Automatica*, vol. 30, no. 7, pp. 1083-1138, 1994.

[3] N. Barahanov and R. Ortega, "Necessary and Sufficient Conditions for Passivity of the LuGre Friction Model," *IEEE Transactions on Automatic Control*, vol. 45, no. 4, pp. 830-832, Apr. 2000.

[4] P. A. Bliman and M. Sorine, "Easy-to-use Realistic Dry Friction Models for Automatic Control," in *Proceedings of the 3rd European. Control Conference,* ECC'95, Rome, Italy, 1995, pp. 3788-3794.

[5] C. Canudas de Wit, H. Olsson, K. J. Astrom, and P. Lischinsky, "A New Model for Control of Systems with Friction," *IEEE Transactions Automatic Control*, vol. 40, pp. 419-425, Mar. 1995.

[6] W. E. Dixon, A. Behal, D. M. Dawson, and S. Nagarkatti, *Nonlinear Control of Engineering Systems: A Lyapunov-Based Approach*, Birkhäuser Boston, 2003.

[7] P. Dahl, *A Solid Friction Model*, The Aerospace Corporation, El Segundo, CA, Tech. Rep. TOR-0158(3107-18), 1968.

[8] P. Dupont, V. Hayward, B. Armstrong, and F. Altpeter, "Single State Elastoplastic Friction Models," *IEEE Transactions Automatic Control*, vol. 47, pp. 683-687, Apr. 2002.

[9] G. Ferretti, G. Magnani, G. Martucci, P. Rocco, V. Stampacchia, *Friction Model Validation in Sliding and Presliding Regimes with High Resolution Encoders*, in Experimental Robotics VIII., B. Siciliano and P. Dario, Eds. New York: Springer-Verlag, 2003, pp. 328-337.

[10] G. Ferretti, G. Magnani, and P. Rocco," Single and Multistate Integral Friction Models," *IEEE Transactions Automatic Control*, vol. 49, pp. 2292-2297, Dec. 2004.

[11] V. Lampaert, J. Swevers, and F. Al-Bender, "Modification of the Leuven Integrated Friction Model Structure," *IEEE Transactions on Automatic Control*, vol. 47, no. 4, pp. 683-687, April 2002.

[12] J. Swevers, F. Al-Bender, C. G. Ganseman, and T. Prajogo," An Integrated Friction Model Structure with Improved Presliding Behavior for Accurate Friction Compensation," *IEEE Transactions Automatic Control*, vol. 45, pp. 675-686, Apr. 2000.

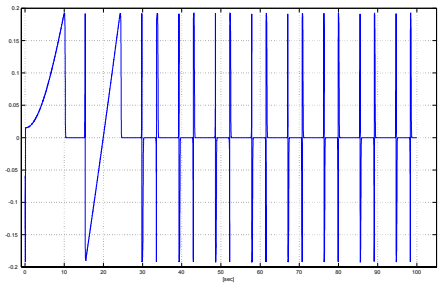

Fig. 16. Friction coefficient vs time.

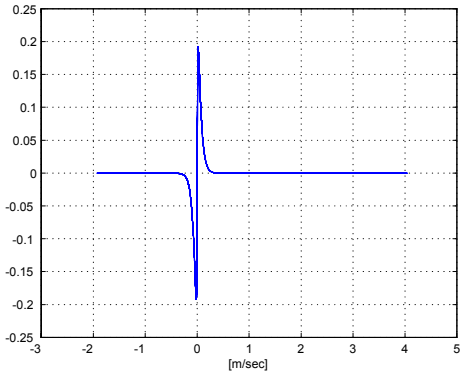

Fig. 17. Friction coefficient vs slip velocity.

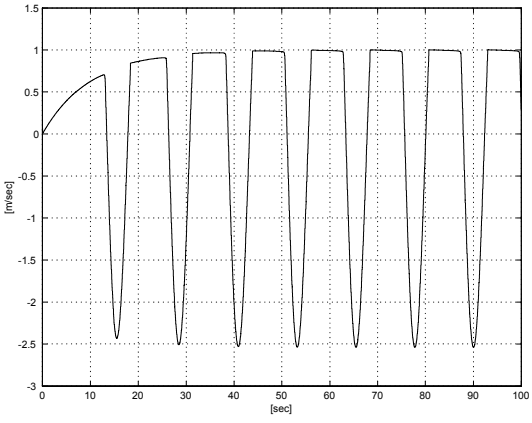

Fig. 18. Block velocity vs time.

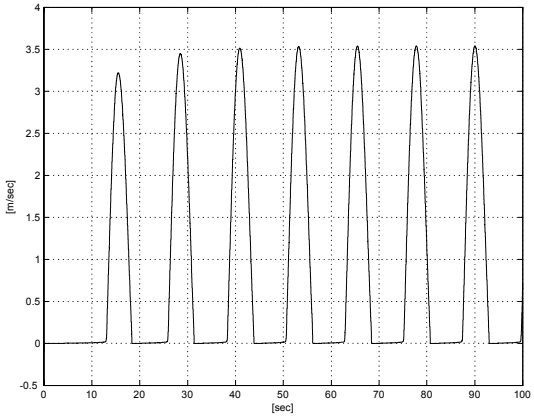

Fig. 19. Slip velocity vs time.

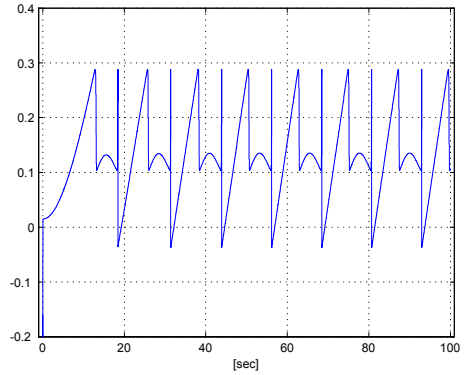

Fig. 20. Friction coefficient vs time.

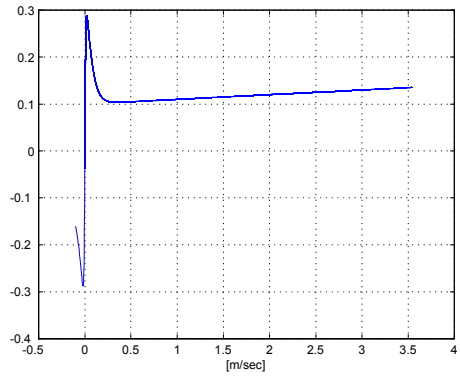

Fig. 21. Friction coefficient vs slip velocity.